Structural comparison of Cu^{II} complexes in atom transfer radical polymerization

Guido Kickelbick,*[a] Tomislav Pintauer[b] and Krzysztof Matyjaszewski*[b]

[a] *Institut für Anorganische Chemie, Techniche Universität Wien, Getreidemarkt 9/153, 1060 Wien, Austria*

[b] *Center for Macromolecular Engineering, Department of Chemistry, Carnegie Mellon University, 4400 Fifth Avenue, Pittsburgh, PA 15213, USA*

Received (in Montpellier, France) 21st June 2001, Accepted 3rd December 2001
First published as an Advance Article on the web

The molecular structures of $[Cu^{II}(dNbpy)_2Br]^+[Cu^{I}Br_2]^-$, $Cu^{II}(pmdeta)Br_2$, $Cu^{II}(tNtpy)Br_2$, $[Cu^{II}(hmteta)Br]^+[Br]^-$ and $[Cu^{II}(cyclam)Br]^+[Br]^-$ [dNbpy = 4,4′-di(5-nonyl)-2,2′-bipyridine, pmdeta = *N*,*N*,*N*′,*N*′,*N*″-pentamethyldiethylenetriamine, tNtpy = 4,4′,4″-tris(5-nonyl)-2,2′:6′,2″-terpyridine, hmteta = 1,1,4,7,10,10-hexamethyltriethylenetetramine, Me_4cyclam = 1,4,8,11-tetraaza-1,4,8,11-tetramethylcyclotetradecane] isolated from atom transfer radical polymerizations (ATRP) were determined. The Cu^{II} complexes showed either a trigonal bipyramidal structure as in the case of the dNbpy ligand, or a distorted square pyramidal coordination in the case of triamines and tetramines. Depending on the type of amine ligand, the complexes were either neutral (triamines) or ionic (bpy and tetramines). The counterions in the case of the ionic complexes were either bromide (Me_4cyclam and hmteta) or the linear $[Cu^{I}Br_2]^-$ anion (dNbpy). No direct correlation was found between the Cu^{II}–Br bond length and the deactivation rate constant in ATRP, which suggests that other parameters such as the entropy for the structural reorganization between the Cu^{I} and Cu^{II} complexes might play an important role in determining the overall activity of the catalyst in ATRP.

Since its discovery in 1995, atom transfer radical polymerization (ATRP) has experienced substantial progress and has become one of the most powerful tools in obtaining well defined polymers by radical means.[1–6] The catalytic cycle in ATRP involves the reversible switching between two oxidation states of a transition metal complex.[7,8] Shown in Scheme 1 is the proposed mechanism for a typical polymerization system using a copper(I) halide/2,2′-bipyridine (bpy) derivative as the catalyst.[9] Homolytic cleavage of the alkyl halide bond (R–X) by the Cu^{I} complex generates an alkyl radical R$^{\bullet}$ and the corresponding Cu^{II} complex. The radical R$^{\bullet}$ can propagate, with a propagation rate constant k_p, by adding across the double bond of a vinyl monomer, terminate by either coupling or disproportionation (k_t), or be reversibly deactivated by the Cu^{II} complex (k_d). Since the equilibrium is strongly shifted towards the dormant species ($k_a \ll k_d$), radical termination is suppressed. As a result of the persistent radical effect,[10,11] polymers with predictable molecular weights, narrow molecular weight distributions and high functionalities can be synthesized.

The equilibrium constant for ATRP ($K_{eq} = k_a/k_d$) shows a strong dependence on the structure of the complexing ligand. Shown in Scheme 2 are some bi-,[2,9] tri-,[12,13] and tetradentate[13,14] nitrogen based ligands typically used for ATRP in our laboratories. In addition, ligands such as pyridineimines[15] and phenanthrolines[16] have also been used. The coordination of the ligand is inherently related to the ability of copper complexes to be oxidized/reduced by the corresponding R–X.[17,18] Consequently, the study of the structures of Cu^{I} and Cu^{II} complexes involved in ATRP could provide further understanding of this catalytic process. This has been recognized in recent structural characterizations of $Cu^{I}Br$ and $Cu^{II}Br_2$ complexes with *n*-alkyl-(2-pyridyl)methanimine ligands.[19,20] Furthermore, structural studies of these ATRP catalysts have provided information on the importance of the solvent and monomer coordination on the catalyst activity.[21] In conjunction with the chemistry and the dynamics associated in the atom transfer step between copper centers, structural and mechanistic studies can also provide much needed

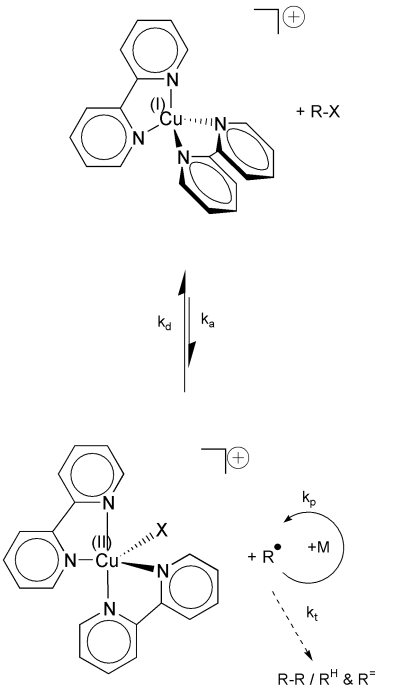

Scheme 1 Proposed mechanism for ATRP.

 DOI: 10.1039/b105454f

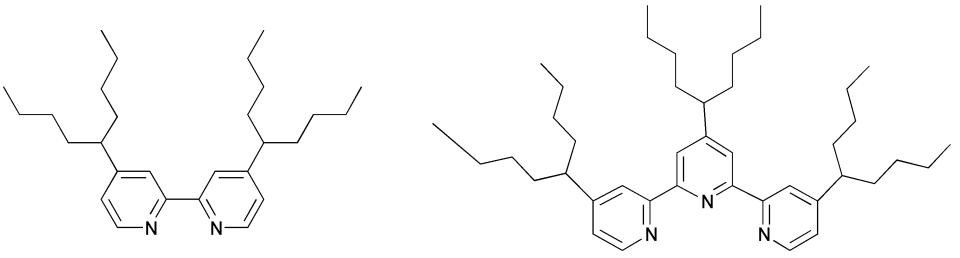

4,4'-di(5-nonyl)-2,2'-bipyridine
dNbpy

4,4',4''-tris(5-nonyl)-2,2':6',2''-terpyridine
tNtpy

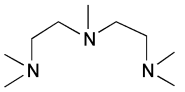

N,N,N',N'',N''-pentamethyldiethylenetriamine
pmdeta

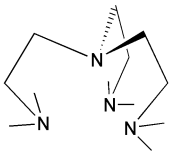

tris[2-(dimethylamino)ethyl]amine
Me_6tren

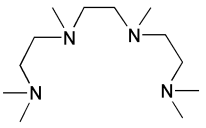

1,1,4,7,10,10-hexamethyltriethylenetetramine
hmteta

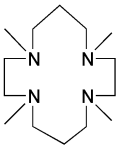

1,4,8,11-tetraaza-1,4,8,11-tetra-
methylcyclotetradecane
Me_4cyclam

Scheme 2 Nitrogen based ligands typically used in ATRP.

information about how to extend polymerization control to even higher molecular weight polymers, develop more active catalysts that can be used at lower concentrations, and polymerize in a controlled fashion less reactive monomers (*e.g.*, vinyl esters and dienes).

In this paper, we report the solid state X-ray structures of Cu^{II} complexes with nitrogen based ligands typically used in our laboratories, which were directly obtained by precipitation from the polymerization solutions. The characterized compounds are expected to be similar to those involved in the ATRP process. The structural changes from Cu^{I} to Cu^{II} complexes, as well as Cu^{II}–Br bond lengths, are discussed as potential parameters for determining the activity of the ATRP active catalysts.

Experimental

Materials

Copper(I) bromide (98% Aldrich) was purified by overnight stirring in glacial acetic acid, filtration under an inert gas atmosphere and washing with excess dry ethanol. Copper(II) bromide (98% Aldrich) was used without further purification. Styrene and methyl acrylate (all Aldrich) were stirred over CaH_2, distilled under reduced pressure and stored in a refrigerator. Acetonitrile, *N*,*N*,*N*′,*N*″,*N*″-pentamethyldiethylenetriamine (pmdeta), 1,1,4,7,10,10-hexamethyltriethylenetetramine (hmteta) and 1,4,8,11-tetraaza-1,4,8,11-tetramethylcyclotetradecane (Me_4cyclam) were purchased from Aldrich and used without further purification. 4,4′-Di(5-nonyl)-2,2′-bipyridine (dNbpy)[22] and 4,4′,4″-tris(5-nonyl)-2,2′:6′,2″-terpyridine (tNtpy)[12] were prepared according to the literature procedures.

All polymerization reactions were carried out under standard literature procedures.[9]

Crystals of the copper complexes were obtained from the polymerization solutions by allowing them to stand at room temperature for at least three days.

X-Ray structure analysis

Crystal data and experimental details are given in Table 1. The X-ray data were collected at room temperature on a Siemens SMART CCD area detector diffractometer using graphite monochromated Mo-Kα radiation ($\lambda = 0.71073$ Å), a nominal crystal-to-detector distance of 4.40 cm and 0.3° ω scan frames. A whole hemisphere of data was collected in all cases. However, due to low scattering intensities in the high theta range, high resolution limits of 1.0 Å were employed for all data sets. Corrections for Lorentz polarization effects and an empirical absorption correction with the program SADABS[23a] were applied. The structures were solved by Patterson and direct methods (SHELXS86[23b]) and refined by the full-matrix least-squares method based on F^2 (SHELXL93[23c]). All non-hydrogen atoms were refined anisotropically and the hydrogens were included in idealized positions.

CCDC reference numbers 181514–181518. See http://www.rsc.org/suppdata/nj/b1/b105454f/ for crystallographic data in CIF or other electronic format.

Results

Bidentate ligands

Cu^{II}/dNbpy. Unsubstituted 2,2′-bipyridine was the first ligand used in copper mediated ATRP.[2] Alkyl substitutions in

Table 1 Crystal data and structure refinement for Cu^{II} complexes

	$[Cu^{II}(dNbpy)Br]^+[CuBr_2]^-$	$Cu^{II}(tNtpy)Br_2$	$Cu^{II}(pmdeta)Br_2$	$[Cu^{II}(Me_4cyclam)Br]^+[Br]^-$	$[Cu^{II}(hmteta)Br]^+[Br]^-$
Empirical formula	$C_{56}H_{88}Br_3Cu_2N_4$	$C_{42}H_{65}Br_2CuN_3$	$C_9H_{23}Br_2CuN_3$	$C_{14}H_{32}Br_2CuN_4$	$C_{12}H_{23}Br_2CuN_4$
Formula weight	1184.11	835.33	396.66	479.80	446.70
Crystal system	Monoclinic	Orthorhombic	Monoclinic	Orthorhombic	Orthorhombic
Space group	$C2/c$	$P2_12_12_1$	$P2_1/c$	$Pca2_1$	$Pca2_1$
a/pm	3494.13(15)	1476.79(3)	1516.4(3)	1528.58(2)	1545.52(4)
b/pm	2481.05(10)	1619.12(4)	1366.4(3)	808.2	808.65(2)
c/pm	1716.80(7)	1886.63(3)	1484.6(3)	1504.21(2)	1461.16(3)
α/°	90.	90.	90.	90.	90.
β/°	95.362(1)	90.	100.35(3)	90.	90.
γ/°	90.	90.	90.	90.	90.
u/pm^3	$14\,818.0 \times 10^6$	4511.12×10^6	3026.1×10^6	1858.28×10^6	1826.14×10^6
Z	8	4	8	4	4
T/K	293(2)	293(2)	293(2)	293(2)	293(2)
μ/mm^{-1}	2.221	2.284	6.704	5.476	5.566
Total reflect.	47847	13414	12426	13501	8433
Indep. reflect.	6500	4702	3171	5265	1008
R_{int}	0.0748	0.0574	0.0378	0.0449	0.0378
R	0.1185	0.0393	0.0252	0.0357	0.0358
R_w	0.3138	0.0858	0.0518	0.0704	0.0988

the 4 and 4′ positions of the bipyridine ring, such as in the dNbpy ligand, further improved the solubility of the catalyst in nonpolar medium, which resulted in higher conversions with polydispersities remaining low.[9,24] The starting Cu^I complex, which is formed by the reaction between Cu^IBr and dNbpy, has a tetrahedral $[Cu^I(dNbpy)_2]^+$ cation and linear $[Cu^IBr_2]^-$ anion. This 1 : 1 stoichiometry between Cu^IBr and dNbpy in nonpolar medium has been confirmed by extended X-ray absorption fine structure (EXAFS)[25] and electrospray ionization mass spectrometry (ESI-MS)[26] measurements.

EXAFS experiments determined that the average Cu^I–N bond length in $[Cu^I(dNbpy)_2]^+$ is 2.00 Å and the average Cu^I–Br bond length in $[Cu^IBr_2]^-$ is 2.25 Å. The average Cu^I–N bond length in the cation is consistent with the Cu^I–N bond lengths in bpy derivatives such as $[Cu^I(bpy)_2]^+[ClO_4]^-$ [27] and $[Cu^I(6,6'\text{-}Me_2\text{-}bpy)_2]^+[BF_4]^-$.[28] Also, the average Cu^I–Br bond length in the linear $[Cu^IBr_2]^-$ anion is similar to that in known complexes such as $[N(C_4H_9)_4]^+[Cu^IBr_2]^-$,[29] $[P(C_6H_5)_4]^+[Cu^IBr_2]^-$ [30] and $[Cu^I(phen)_2]^+[Cu^IBr_2]^-$.[31]

ESI-MS spectra of Cu^IBr complexed with 1 or 2 equivalents of dNbpy in toluene, methyl acrylate or styrene showed the presence of only the $[Cu^I(dNbpy)_2]^+$ cation and $[Cu^IBr_2]^-$ anion. The $[Cu^IBr_2]^-$ anions in the system indicate the binding competition between dNbpy and bromine ligand towards the Cu^I center. Other anions such as $[Br]^-$ could also be present in the Cu^IBr/(2)dNbpy system, but could not be detected using available ESI-MS equipment. Recently, the molecular structure of a related bpy based ATRP active catalyst, $[Cu^I(dNEObpy)_2][Cu^IBr_2]$ [dNEObpy = 4,4′-bis(neophyldimethylsilylmethyl)-2,2′-bipyridine], further confirmed this unusual 1 : 1 stoichiometry in nonpolar medium between Cu^IBr and bpy based ligands.[32]

The solid state X-ray structure of isolated crystals obtained from a bulk polymerization of methyl acrylate catalyzed by Cu^IBr/2dNbpy is shown in Fig. 1. The obtained structure shows a trigonal bipyramidal $[Cu^{II}(dNbpy)_2Br]^+$ cation and linear $[Cu^IBr_2]^-$ anion. The shortest distance between the bromine atom of the anion (Br2) and the copper center of the cation (Cu1) is 6.182 Å, which rules out the possibility of the formation of semicoordinate Cu–Br bonds. The Cu^{II}–N [1.946(13), 2.051(15), 1.977(15) and 2.088(16) Å] and Cu^{II}–Br [2.426(3) Å] bond lengths (Table 2) of the $[Cu^{II}(dNbpy)_2Br]^+$ cation are typical for a distorted trigonal bipyramidal geometry and are comparable to those of related bpy complexes with the general formula $[Cu^{II}(bpy)Br]^+[Y]^-$ ($Y = PF_6$, CF_3SO_3, ClO_4, *etc.*).[33]

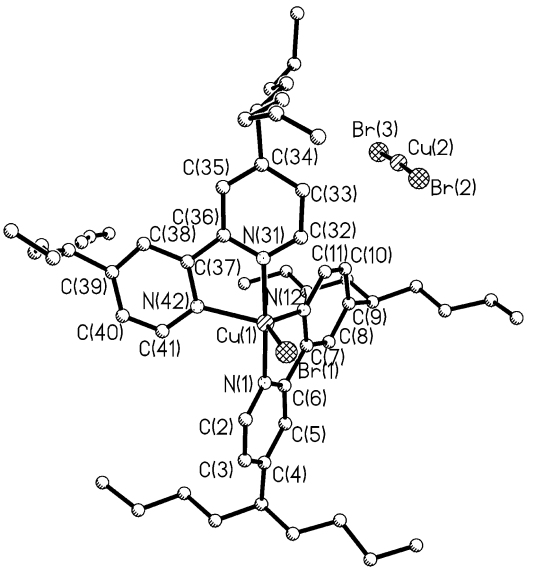

Fig. 1 Molecular structure of the complex $[Cu^{II}(dNbpy)_2Br]^+[Cu^IBr_2]^-$.

The molecular structure of an isolated $[Cu^{II}(dNbpy)_2Br]^+[Cu^IBr_2]^-$ complex might not exactly describe the structure in solution, taking into account the possibility that more than one species may coexist in equilibrium. For example, in nonpolar media, the square planar complex $Cu^{II}(dNbpy)Br_2$ has been observed.[34] However, it is plausible to assume that the $[Cu^{II}(dNbpy)_2Br]^+[Cu^IBr_2]^-$ complex was formed by the abstraction of a bromine atom from an alkyl halide by a

Table 2 Selected bond distances (Å) and angles (deg) for $[Cu^{II}(dNbpy)_2Br]^+[Cu^IBr_2]$

Br(1)–Cu(1)	2.426(3)	N(12)–Cu(1)–N(31)	94.7(6)
Cu(1)–N(1)	1.946(13)	N(1)–Cu(1)–N(42)	98.2(7)
Cu(1)–N(31)	1.977(15)	N(31)–Cu(1)–N(42)	78.0(7)
Cu(1)–N(12)	2.051(15)	N(12)–Cu(1)–N(42)	112.1(6)
Cu(1)–N(42)	2.088(16)	N(1)–Cu(1)–Br(1)	94.5(4)
Cu(2)–Br(2)	2.216(4)	Br(1)–Cu(1)– N(31)	92.7(5)
Cu(2)–Br(3)	2.218(4)	Br(1)–Cu(1)–N(12)	131.1(4)
N(1)–Cu(1)–N(31)	172.8(7)	Br(1)–Cu(1)–N(42)	116.7(4)
N(1)–Cu(1)–N(12)	80.9(6)	Br(2)–Cu(2)–Br(3)	176.57(17)

tetrahedral $[Cu^{I}(dNbpy)_2]^+$ cation in the $[Cu^{I}(dNbpy)_2]^+$ $[Cu^{I}Br_2]^-$ complex, as indicated in Scheme 1. The role of the $[Cu^{I}Br_2]^-$ anions in the system is still not fully understood. Although they are not active in ATRP,[9,32] they could affect the geometry of the Cu^{I} and Cu^{II} cations, and therefore directly influence their ability to be oxidized and reduced by the corresponding alkyl halide and alkyl radical, respectively.

Tridentate ligands

Cu^{II}/pmdeta. Apart from substituted bipyridines, other linear and cyclic amines were successfully used as ligands for ATRP catalysts.[13,14,35,36] Particularly, the commercially available tridentate *N*,*N*,*N*′,*N*″,*N*″-pentamethyldiethylenetriamine (pmdeta) showed a high potential for the controlled polymerization of a variety of monomers. Typically, the ligand to copper(I) halide ratio used in the polymerization was 1 : 1. The structure of the $Cu^{I}Br$/pmdeta complex is not known. Recently, we investigated this system using EXAFS measurements on both the copper and bromine edges.[37] The results were inconclusive and the two possible structures included neutral tetrahedral $[Cu^{I}(pmdeta)Br]$ and an ionic $[Cu^{I}(pmdeta)]^+[Cu^{I}Br_2]^-$ complex. Suitable crystals of the complex for the X-ray analysis could not be obtained and further experimental evidence is needed to confirm the nature and bonding of pmdeta to $Cu^{I}Br$.

In Fig. 2 is shown the molecular structure of $[Cu^{II}(pmdeta)Br_2]$, which precipitated from the ATRP of methyl acrylate catalyzed by $Cu^{I}Br$/pmdeta. The complex has a square pyramidal coordination sphere with three nitrogens and one bromine situated in the basal plane and the second bromine in the apical position. Selected bond lengths and angles are shown in Table 3.

The Cu^{II}–Br bond length in the apical position [2.6442(9) Å] is much longer than the Cu^{II}–Br bond length in the basal position [2.4462(9) Å]. This is due to the relatively small energy differences between the trigonal bipyramidal and square pyramidal geometries of pentacoordinated Cu^{II} complexes.[38] The cleavage of the Cu^{II}–Br bond by the corresponding radical in the deactivation process of ATRP (Scheme 1) is therefore expected to occur in the apical position because it is energetically more favorable.

The methyl groups in the pmdeta ligand also have an influence on the structure of the Cu^{II} complex. While the H substituted triamine forms dimers,[39] the methyl substituted ligand shows discrete molecules. A similar behavior has been observed for the chlorine derivatives.[40–42]

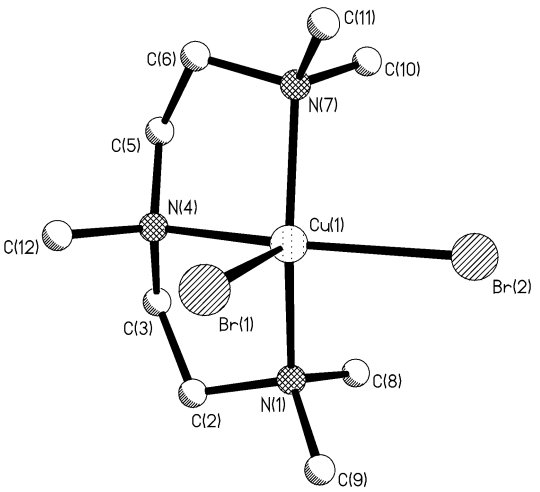

Fig. 2 Molecular structure of $[Cu^{II}(pmdeta)Br_2]$.

Table 3 Selected bond distances (Å) and angles (deg) for $[Cu^{II}(pmdeta)Br_2]$

Cu(1)–N(1)	2.086(4)	N(1)–Cu(1)–Br(2)	91.36(11)
Cu(1)–N(7)	2.103(4)	N(7)–Cu(1)–Br(2)	92.17(11)
Cu(1)–N(4)	2.104(4)	N(4)–Cu(1)–Br(2)	165.65(11)
Cu(1)–Br(2)	2.4462(9)	N(1)–Cu(1)–Br(1)	103.18(11)
Cu(1)–Br(1)	2.6442(9)	N(7)–Cu(1)–Br(1)	105.16(11)
N(1)–Cu(1)–N(7)	150.59(16)	N(4)–Cu(1)–Br(1)	95.98(11)
N(1)–Cu(1)–N(4)	84.68(15)	Br(2)–Cu(1)–Br(1)	98.35(3)
N(7)–Cu(1)–N(4)	84.73(15)		

Cu^{II}/tNtpy. The substituted terpyridine, 4,4′,4″-tris(5-nonyl)-2,2′:6′,2″-terpyridine (tNtpy), is a planar tridentate ligand that was successfully used in the homogeneous ATRP of methyl acrylate and styrene. The polymerization of both monomers was controlled and the resulting polymers had relatively narrow polydispersities ($M_w/M_n < 1.2$).[12] Similar to pmdeta, the typical ligand to copper(I) halide ratio used in the polymerization was 1 : 1. The molecular structure of the neutral $[Cu^{II}(tNtpy)Br_2]$ complex that was precipitated from ATRP of styrene catalyzed by $Cu^{I}Br$/tNtpy is shown in Fig. 3. The complex has distorted square pyramidal geometry and is coordinated by three nitrogen atoms of the tNtpy ligand and two bromine atoms. Selected bond lengths and angles are given in Table 4.

Analogous to the molecular structure of $[Cu^{II}(pmdeta)Br_2]$, the Cu^{II}–Br bond length in the apical position [2.5276(10) Å] is longer than the Cu^{II}–Br bond length in the basal position [2.4071(10) Å]. Consequently, the deactivation process is more likely to occur by the cleavage of the bromine bond in the apical position. The elongation of the Cu^{II}–Br bond in the apical position could be attributed to the small energy difference between the trigonal bipyramidal and square pyramidal geometry of the $[Cu^{II}(tNtpy)Br_2]$ complex as discussed above. Another possibility includes the steric hindrance of the complex imposed by the long alkyl chains in the terpyridine ligand, which affect the crystal packing in the unit cell. This phenomena has not been observed in the molecular structure

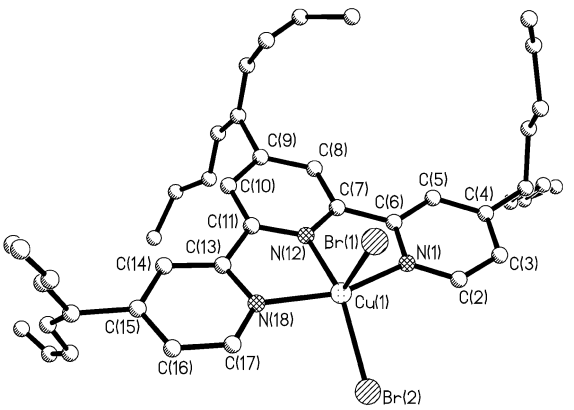

Fig. 3 Molecular structure of $[Cu^{II}(tNtpy)Br_2]$.

Table 4 Selected bond distances (Å) and angles (deg) for $Cu^{II}(tNtpy)Br_2$

Cu(1)–N(12)	1.962(5)	Br(2)–Cu(1)–N(12)	144.43(13)
Cu(1)–N(1)	2.056(5)	N(1)–Cu(1)–Br(2)	98.31(15)
Cu(1)–N(18)	2.062(5)	Br(2)–Cu(1)–N(18)	97.66(15)
Cu(1)–Br(1)	2.5276(10)	Br(1)–Cu(1)–N(12)	105.27(13)
Cu(1)–Br(2)	2.4071(10)	Br(1)–Cu(1)–N(1)	92.03(13)
N(1)–Cu(1)– N(12)	78.7(2)	Br(1)–Cu(1)–N(18)	97.47(13)
N(12)–Cu(1)–N(18)	78.9(2)	Br(1)–Cu(1)–Br(2)	110.26(4)
N(1)–Cu(1)–N(18)	157.3(2)		

of the unsubstituted terpyridine complex [Cu^{II}(tpy)Br_2], where Cu^{II}–Br bond distances were equal (2.493 Å).[43]

Without a knowledge of the structure of the Cu^{I}Br/tNtpy complex, it is difficult to precisely explain the formation of [Cu^{II}(tNtpy)Br_2]. One possibility would include the homolytic cleavage of the alkyl bromide bond by the neutral [Cu^{I}(tNtpy)Br] complex. More experimental evidence is needed to further investigate this system.

Tetradentate ligands

Cu^{II}/hmteta. 1,1,4,7,10,10-Hexamethyltriethylenetetramine (hmteta) is a tetradentate amine ligand that was successfully used in ATRP of styrene, methyl acrylate and methyl methacrylate. The ligand to Cu^{I}Br ratio used in the polymerization was 1 : 1. The structure and the stochiometry of the Cu^{I}Br/hmteta complex are not known. Possible structures include ionic [Cu^{I}(hmteta)]$^+$[Br]$^-$ and [Cu^{I}(hmteta)]$^+$[$Cu^{I}Br_2$]$^-$ complexes. The latter one is supported by the recently published solid state structure of the chlorine derivative [Cu^{I}(hmteta)]$^+$[$CuCl_2$]$^-$.[44] In Fig. 4 is shown the molecular structure of the Cu^{II} complex that was isolated from ATRP of methyl acrylate catalyzed by Cu^{I}Br/hmteta. Selected bond lengths and angles are listed in Table 5.

The complex has a distorted square pyramidal geometry. The Cu^{II}–Br bond length [2.6027(18) Å] in [Cu^{II}(hmteta)Br]-[Br] is similar to that in other square pyramidal Cu^{II} complexes with [Cu^{II}(tetramine)Br]$^+$ chromophores.[45] The distance between the bromine anion and the Cu^{II} center in [Cu^{II}(hmteta) Br]$^+$[Br]$^-$ is 4.645 Å, which indicates that the anion is noncoordinating.

Cu^{II}/Me_4cyclam. Me_4cyclam is the only tetradentate cyclic amine that was investigated in ATRP. The ligand to Cu^{I}Br ratio typically used was 1 : 1. The molecular structure of the corres- ponding Cu^{II} complex that was precipitated from ATRP is shown in Fig. 5. Selected bond lengths and distances are given in Table 6.

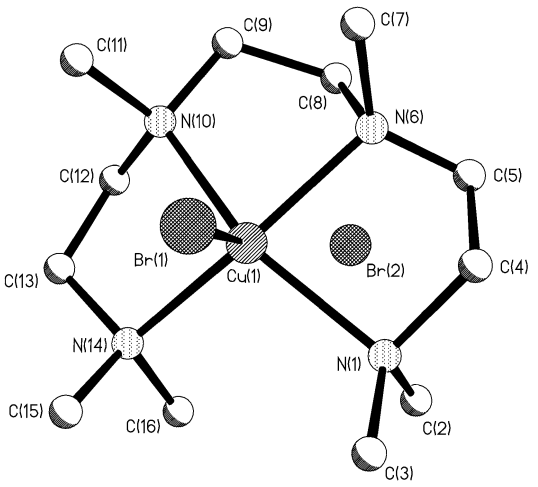

Fig. 4 Molecular structure of [Cu^{II}(hmteta)Br]$^+$[Br]$^-$.

Table 5 Selected bond distances (Å) and angles (deg) for [Cu^{II}(hmteta)Br]$^+$[Br]$^-$

Cu(1)–N(6)	2.082(12)	N(1)–Cu(1)–N(6)	82.0(8)
Cu(1)–N(10)	2.082(12)	N(1)–Cu(1)–N(10)	154.8(7)
Cu(1)–N(14)	2.103(10)	N(1)–Cu(1)–N(14)	101.4(7)
Cu(1)–N(1)	2.167(17)	Br(1)–Cu(1)–N(6)	98.9(3)
Cu(1)–Br(1)	2.6027(18)	Br(1)–Cu(1)–N(10)	103.1(3)
N(6)–Cu(1)–N(10)	82.9(7)	Br(1)–Cu(1)–N(14)	102.7(3)
N(6)–Cu(1)–N(14)	157.3(5)	N(1)–Cu(1)–Br(1)	99.0(5)
N(10)–Cu(1)–N(14)	85.4(6)		

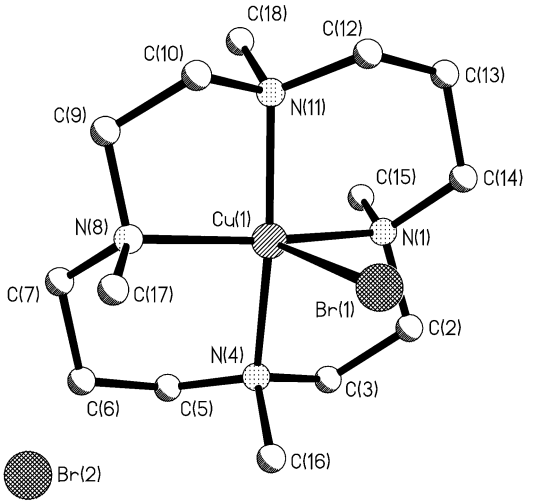

Fig. 5 Molecular structure of [Cu^{II}(Me_4cyclam)Br]$^+$[Br]$^-$.

Table 6 Selected bond distances (Å) and angles (deg) for [Cu^{II}(Me_4cyclam)Br]$^+$[Br]$^-$

Cu(1)–N(11)	2.071(3)	N(1)–Cu(1)–N(4)	86.13(13)
Cu(1)–N(1)	2.078(3)	N(11)–Cu(1)–N(8)	86.66(13)
Cu(1)–N(4)	2.098(3)	N(1)–Cu(1)–N(8)	167.35(13)
Cu(1)–N(8)	2.101(3)	N(4)–Cu(1)–N(8)	93.86(13)
Cu(1)–Br(1)	2.8092(6)	N(11)–Cu(1)–Br(1)	95.22(9)
N(11)–C(12)	1.482(5)	N(1)–Cu(1)–Br(1)	96.04(10)
N(11)–Cu(1)–N(1)	90.58(13)	N(4)–Cu(1)–Br(1)	97.42(9)
N(11)–Cu(1)–N(4)	167.21(13)	N(8)–Cu(1)–Br(1)	96.50(9)

The [Cu^{II}(Me_4cyclam)Br]$^+$[Br]$^-$ complex is square pyramidal in geometry and the Cu^{II}–Br bond length is 2.8092(6) Å. The geometry of the cation is consistent with both chlorine and iodine derivatives.[46–48] The shortest distance between the [Br]$^-$ anion and [Cu^{II}(Me_4cyclam)Br]$^+$ cation is 4.349 Å, which indicates no substantial interaction and rules out the possibility for semicoordination in the solid state.

Discussion

Another tetradentate nitrogen based ligand that was successfully used in ATRP is tris[2-(dimethylamino)ethyl]amine (Me_6tren). Typically, the ligand to Cu^{I}Br ratio was 1 : 1. This catalytic system showed a very high activity, enabling fast and controlled polymerization of methyl acrylate at ambient temperature.[14] The molecular structure of the isolated Cu^{II} complex that was formed during the polymerization indicated an ionic [Cu^{II}(Me_6tren)Br]$^+$[Br]$^-$ complex. The complex was distorted trigonal bipyramidal in geometry and the average Cu^{II}–Br bond length was 2.393(3) Å. All other bond lengths and angles were in full agreement with the previously reported molecular structure of [Cu^{II}(Me_6tren)Br]$^+$[Br]$^-$.[49]

The isolated and characterized Cu^{II} complexes presented in this study show either a trigonal bipyramidal structure as in the case of the dNbpy ligand, or a distorted square pyramidal coordination in the case of triamines and tetramines. Depending on the type of amine ligand, the complexes are either neutral (triamines) or ionic (bpy and tetramines). The counterions in the case of the ionic complexes are either bromide (Me_4cyclam and hmteta) or the linear [$Cu^{I}Br_2$]$^-$ anion (dNbpy).

Table 7 Comparison of the Cu^{II}–Br bond length in the Cu^{II} complexes with the deactivation rate constant in the ATRP equilibrium. Only the bond lengths of the cations are considered

Complex	Cu^{II}–Br/Å	$k_{deact}/M^{-1}\ s^{-1}$	Ref.
$[Cu^{II}(Me_6tren)Br]^+[Br]^-$	2.393(3)	1.4×10^7 [a]	49,51
$[Cu^{II}(dNbpy)Br]^+[Cu^{I}Br_2]^-$	2.426(3)	2.5×10^7 [a]	51
$Cu^{II}(tNtpy)Br_2$	2.5276(10) *2.4071(10)*	4.1×10^5 [a]	53
$Cu^{II}(pmdeta)Br_2$	2.6442(9) *2.4462(9)*	6.1×10^6 [a]	51
$[Cu^{II}(Me_4cyclam)Br]^+[Br]^-$	2.8092(6)	2.0×10^4 [b]	52

[a] Rate constant measured in CH_3CN at 75 °C using 1-phenylethyl radical. [b] Rate constant estimated by the degree of polymerization of poly(styrene) formed by initiation with AIBN in the presence of $CuBr_2$/Me_4cyclam and 1-phenylethyl bromide.

The structures of the Cu^I and Cu^{II} complexes that are involved in the ATRP equilibrium play an important role in determining the overall activity of the catalyst. Previously, this activity has been correlated with properties such as the redox potential,[50] and more recently the activation and deactivation rate constants.[51–53] Additionally, factors such as the polarity of both the monomers and the reaction medium are also related to the catalyst activity. The simplest structural parameter that can be correlated with the kinetics of the ATRP deactivation process is the Cu^{II}–Br bond length. The strength of this bond could be used as a crude estimate to evaluate the deactivation rate constant, which is responsible for the control of ATRP systems. In Table 7 is shown the comparison between the Cu^{II}–Br bond length and the deactivation rate constant for the Cu^{II} complexes with Me_6tren,[49] dNbpy, tNtpy, pmdeta and Me_4cyclam.

As indicated in the table, there is no direct correlation between the length of the Cu^{II}–Br bond and the deactivation rate constant. It seems that a weaker or longer Cu^{II}–Br bond length is not the only factor that affects the deactivation rate constant. The structural reorganization of the Cu^{II} complex upon bromine abstraction by the corresponding radical is another important process that needs to be taken into account. Without a knowledge of the structures of the Cu^I complexes in ATRP, it is difficult to predict the entropies for this reorganization. Additional factors that need to be taken into account include the ligand basicity and overall stability constants of the Cu^I and Cu^{II} complexes.[54] Other experimental techniques such as EXAFS, UV-Vis, NMR and far-IR could provide such information and are currently being carried out.

Conclusions

The molecular structures of $[Cu^{II}(dNbpy)Br]^+[Cu^IBr_2]^-$, $Cu^{II}(pmdeta)Br_2$, $Cu^{II}(tNtpy)Br_2$, $[Cu^{II}(hmteta)Br]^+[Br]^-$ and $[Cu^{II}(Me_4cyclam)Br]^+[Br]^-$ that were isolated from the ATRP solutions were determined. The Cu^{II} complexes showed either a trigonal bipyramidal structure in the case of the dNbpy ligand, or a distorted square pyramidal coordination in the case of triamines and tetramines. The Cu^{II}–Br bond length in the complexes could not be directly correlated with the deactivation rate constant in the ATRP equilibrium. Other contributions such as entropy for the structural reorganization from Cu^{II} to Cu^I complex and *vice versa* must also play an important role in determining the activity of the Cu complexes in ATRP, and are currently under investigation.

Acknowledgements

The financial support from the CMU ATRP Consortium, NSF (CHE-0096601) and Fonds zur Förderung der wissenschaftlichen Forschung-Vienna, Austria is greatly appreciated.

References

1 M. Kato, M. Kamigaito, M. Sawamoto and T. Higashimura, *Macromolecules*, 1995, **28**, 1721.
2 J.-S. Wang and K. Matyjaszewski, *J. Am. Chem. Soc.*, 1995, **117**, 5614.
3 *Controlled Radical Polymerization*, ed. K. Matyjaszewski, ASC Symposium Series, ACS, Washington, DC, 1998.
4 *Controlled/Living Radical Polymerization: Progress in ATRP, NMP and RAFT*, ed. K. Matyjaszewski, ASC Symposium Series, ACS, Washington, DC, 2000.
5 T. E. Patten and K. Matyjaszewski, *Adv. Mater.*, 1998, **10**, 901.
6 K. Matyjaszewski and J. Xia, *Chem. Rev.*, 2001, **101**, 2921.
7 K. Matyjaszewski, *Chem. Eur. J.*, 1999, **5**, 3095.
8 T. E. Patten and K. Matyjaszewski, *Acc. Chem. Res.*, 1999, **32**, 895.
9 K. Matyjaszewski, T. E. Patten and J. Xia, *J. Am. Chem. Soc.*, 1997, **119**, 674.
10 H. Fischer, *Macromolecules*, 1997, **30**, 5666.
11 H. Fischer, *J. Polym. Sci., Part A: Polym. Chem.*, 1999, **37**, 1885.
12 G. Kickelbick and K. Matyjaszewski, *Macromol. Rapid Commun.*, 1999, **20**, 341.
13 J. Xia and K. Matyjaszewski, *Macromolecules*, 1997, **30**, 7697.
14 J. Xia, S. G. Gaynor and K. Matyjaszewski, *Macromolecules*, 1998, **31**, 5958.
15 D. M. Haddleton, C. B. Jasieczek, M. J. Hannon and A. J. Shooter, *Macromolecules*, 1997, **30**, 2190.
16 M. Destarac, J. M. Bassiere and B. Boutevin, *Macromol. Rapid Commun.*, 1997, **18**, 967.
17 E. A. Ambundo, M. V. Deydier, A. J. Grall, N. Aguera-Vega, L. T. Dressel, T. H. Cooper, M. J. Heeg, L. A. Ochrymowycz and D. B. Rorabacher, *Inrorg. Chem.*, 1999, **38**, 4233.
18 A. J. Clark, G. M. Battle, A. M. Heming, D. M. Haddleton and A. Bridge, *Tetrahedron Lett.*, 2001, **42**, 2003.
19 D. M. Haddleton, A. J. Clark, D. J. Duncalf, A. M. Heming, D. Kukulj and A. J. Shooter, *J. Chem. Soc., Dalton Trans.*, 1998, 381.
20 D. M. Haddleton, D. J. Duncalf, D. Kukulj, M. C. Crossman, S. G. Jackson, S. A. F. Bon, A. J. Clark and A. J. Shooter, *Eur. J. Inrog. Chem.*, 1998, 1799.
21 D. M. Haddleton, S. Perrier and S. A. F. Bon, *Macromolecules*, 2000, **33**, 8246.
22 T. B. Hadda and H. J. Bozec, *Polyhedron*, 1988, **7**, 575.
23 (*a*) G. Sheldrick, SADABS, Program for Siemens Area Detector Absorption Correction, Universität Göttingen, Germany, 1996; (*b*) G. Sheldrick, *Acta Crystallogr., Sect. A*, 1995, **51**, 33; (*c*) G. Sheldrick, SHELXL93 SADABS, Program for Siemens Area Detector Absorption Correction, Universität Göttingen, Germany, 1993.
24 T. E. Patten, J. Xia, T. Abernathy and K. Matyjaszewski, *Science*, 1996, **272**, 866.
25 G. Kickelbick, U. Reinhol, T. S. Ertel, A. Weber, H. Bertagnolli and K. Matyjaszewski, *Inorg. Chem.*, 2001, **40**, 6.
26 T. Pintauer, C. B. Jasieczek and K. Matyjaszewski, *J. Mass. Spectrom.*, 2000, **35**, 1295.
27 M. Munakata, S. Kitagawa, A. Asahara and H. Masuda, *Bull. Chem. Soc. Jpn.*, 1987, **60**, 1927.
28 P. J. Burke, D. R. McMillin and W. R. Robinson, *Inorg. Chem.*, 1980, **19**, 1211.
29 M. Asplund, S. Jagner and M. Nilsson, *Acta Chem. Scand., Ser. A*, 1983, **37**, 57.
30 S. Anderson and S. Jagner, *Acta Chem. Scand., Ser. A*, 1985, **39**, 297.
31 P. C. Healy, L. M. Engelhardt, V. A. Patrick and A. H. White, *J. Chem. Soc., Dalton Trans.*, 1985, 2541.
32 A. T. Levy, M. M. Olmstead and T. E. Patten, *Inorg. Chem.*, 2000, **39**, 1628.
33 C. O'Sullivan, G. Murphy, B. Murphy and B. Hathaway, *J. Chem. Soc., Dalton Trans.*, 1999, 1835.
34 T. Pintauer, J. Qiu, G. Kickelbick and K. Matyjaszewski, *Inorg. Chem.*, 2001, **40**, 2818.
35 J. Xia and K. Matyjaszewski, *Macromolecules*, 1999, **32**, 2434.
36 J. Xia, X. Zhang and K. Matyjaszewski, in *Transition Metal Catalysis in Macromolcular Design*, eds. L. S. Boffa and B. M. Novak, American Chemical Society, Washington, D. C., 2000, vol. 760, p. 207–223.
37 T. Pintauer, U. Reinohl, M. Feth, U. Bertagnolli, K. Matyjaszewski, unpublished results.
38 B. J. Hathaway, *Struct. Bonding*, 1973, **14**, 49.
39 D. K. Towel, S. K. Hoffmann, W. E. Hatfield, P. Singh, P. Chaudhuri and K. Wieghart, *Inorg. Chem.*, 1985, **24**, 4393.

40 S. K. Hoffmann, D. K. Towle, W. E. Hatfield, K. Wieghardt, P. Chaudhuri and J. Weiss, *Mol. Cryst. Liq. Cryst.*, 1984, **107**, 161.
41 M. K. Urtiaga, M. I. Arriortua, R. Cortes and T. Rojo, *Acta Crystalogr., Sect. C*, 1996, **52**, 3007.
42 S. R. Breeze and S. Wang, *Inorg. Chem.*, 1996, **35**, 3404.
43 M. I. Arriortua, J. L. Mesa, T. Rojo, T. Debaerdemaeker, D. Beltran-Porter, H. Stratemeier and D. Reinen, *Inorg. Chem.*, 1988, **27**, 2976.
44 M. Becker, F. W. Heinemann, F. Knoch, W. Donaubauer, G. Liehr, S. Schindler, G. Golub, H. Cohen and D. Meyerstein, *Eur. J. Inorg. Chem.*, 2000, 719.
45 M. F. C. Ladd and D. H. G. Perrins, *Z. Kristallogr.*, 1981, **154**, 155.
46 J. M. Harrowfield, A. M. Sargeson, B. W. Skelton and A. H. White, *Aust. J. Chem.*, 1994, **47**, 181.
47 X. Chen, G. Long, R. D. Willett, T. Hawks, S. Molnar and K. Brewer, *Acta Crystallogr., Sect. C*, 1996, **52**, 1924.
48 T. Heinlein and K.-F. Tebbe, *Z. Kristallogr.*, 1985, **170**, 70.
49 M. D. Vaira and P. L. Orioli, *Acta Crystallogr., Sect. B*, 1968, **24**, 595.
50 J. Qiu, K. Matyjaszewski, L. Thouin and C. Amatore, *Macromol. Chem. Phys.*, 2000, **201**, 1625.
51 K. Matyjaszeski, H.-J. Paik, P. Zhou and S. J. Diamanti, *Macromolecules*, 2001, **34**, 5125.
52 J. Gromada, K. Matyjaszewski, unpublished results.
53 K. Matyjaszewski, B. Gobelt, H.-J. Paik and C. P. Horwitz, *Macromolecules*, 2001, **34**, 430.
54 M. Schatz, M. Becker, F. Thaler, F. Hampel, S. Schindler, R. R. Jacobson, Z. Tyeklar, N. N. Murthy, P. Ghosh, Q. Chen, J. Zubieta and K. D. Karlin, *Inorg. Chem.*, 2000, **40**, 2312.